wave velocity relative to the gas, and the duct is assumed to behave as a half-wave resonator. Therefore, the product of the measured frequency and twice the duct length does not yield the average wave velocity, but rather this latter quantity multiplied by a factor of $(1 - M^2)$. For a resonant frequency of 730 cps, a duct length of 2 ft, and an average wave velocity of 3360 fps, the Mach number as determined from the previous equations is 0.367. Since the nozzle entrance Mach number on the motors used in these tests is 0.45, and the duct length includes the convergent portion of the nozzle, the average Mach number as determined from the resonant frequency appears to be reasonable.

It is obvious that for low Mach numbers and large contraction ratios the effect on the resonant frequency is small, but as the Mach number increases, the reduction in natural or resonant frequency increases. If one has a beforehand knowledge of the wave velocity relative to the gas, say 3360 fps, and uses simple acoustic theory ($M = 0$), the resonant frequency for a 2-ft chamber would be 840 cps. As the Mach number is increased to 0.367, a 13% decrease in resonant frequency is noted.

An important conclusion to be derived from the foregoing discussion is that acoustic theories will not give accurate quantitative results of the analysis of wave oscillations in rocket motors, especially those having small contraction ratios with resultant high Mach number profiles.

References

[1] Burstein, S., Hammer, S., and Agosta, V. D., "Spray combustion model with droplet breakup: analytical and experimental results," *ARS Progress in Astronautics and Rocketry: Detonation and Two-Phase Flow*, edited by S. S. Penner and F. A. Williams (Academic Press, Inc., New York, 1962), Vol. 6, pp. 243–268.

[2] Peschke, W. and Hammer, S., "Pressure gradients in a liquid propellant rocket motor: effect of injector configuration," AIAA J. 2, 1467–1469 (1964).

[3] Agosta, V. D. and Mazzitelli, D. A., "A theoretical study of the vibratory forcing functions in axial flow turbo-jet engines due to flow pulsations," Wright Air Development Center TR 56-74 (January 1956).

Stagnation Equilibrium Layer in Nonequilibrium Blunt-Body Flows

RAUL J. CONTI*
Stanford University, Stanford, Calif.

Introduction

IN 1962, Swigart[1] introduced a novel technique for analyzing inviscid perfect gas flows over blunt bodies in hypersonic flight. The present investigation makes use of this technique to study nonequilibrium flows, and in this paper attention is drawn to the equilibrium layer that exists near the body. Before pursuing this point any further, a brief discussion of the method is included.

The technique in question has been called the method of successive truncations. Its framework is a scheme of systematic approximations where each approximation is rendered solvable by truncation of infinite series. These series are expansions of the flow variables in powers of the curvilinear coordinate leading away from the axis of symmetry of the flow. Thus, for the plane flow field behind a circular-cylindrical shock, Swigart works with the stream function and density (ψ and ρ) which are expanded as (see Fig. 1)

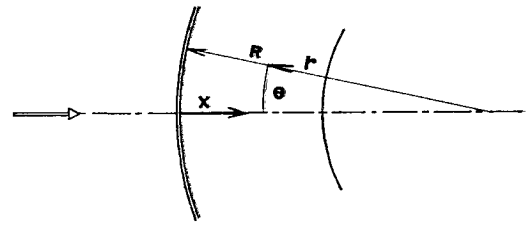

Fig. 1 Circular-cylindrical coordinate system.

$$\psi(r,\theta) = \psi_1(r)\sin\theta + \psi_2(r)\sin^3\theta + O(\sin^5\theta) \quad (1a)$$

$$\rho(r,\theta) = \rho_1(r) + \rho_2(r)\sin^2\theta + O(\sin^4\theta) \quad (1b)$$

The assumption is made that this representation for ψ and ρ is valid for all θ of interest. Then, substitution of the expansions into the governing partial differential equations and equating of like powers of $\sin\theta$ yields sets of ordinary differential equations for the quantities ψ_i, ρ_i. The first-order set, or first-order problem, is defined by two ordinary differential equations for ψ_1, ρ_1, and ρ_2. The appearance of ρ_2 in the first-order problem is due to the ellipticity of the governing partial differential equations and brings about the necessity for some other means of determining ρ_2. One such means is truncation of expansions (1) at the first term, i.e., setting $\rho_2 = 0$.† This renders the first-order problem solvable, but also introduces an approximation in the results. A similar situation occurs in higher-order problems, which are also solved by truncation, thereby creating the successive-approximation character of the method in question.

In the method of successive truncations, each truncation level can be regarded as postulating the θ variation of the flow variables and solving for the r variation. In this light, it is obviously desirable to make a good guess for the θ variation [i.e., assume the proper form for expansions (1)]. This has the double effect of giving good results locally and extending the θ range of validity of the particular truncation being solved. It is presently suggested that this is not easy to do when the density is used as a variable, since density is expected to be nearly constant in the immediate vicinity of the shock and to vary as $(\cos\theta)^{2/\gamma}$ near the body according to the Newtonian approximation. It is clear that no single function of θ will represent the proper density variation both near the shock and near the body. This is perhaps the reason for the poor results exhibited in the first truncation of Ref. 1 for the case at hand (flow behind a circular-cylindrical shock). Here the density behavior at the shock was retained, as can be seen from expansion (1b) in which the first term is independent of θ. On the other hand, a variable that is much more accurately expressible as a function of r times a function of θ is the pressure, which can be expanded as

$$p(r,\theta) = p_1(r)\cos^2\theta + O(\sin^2\theta) \quad (2)$$

which exhibits the cosinusoidal-square variation that is actually expected both near the shock and near the body in hypersonic flow. It is suggested that the use of expansion (2) rather than (1b), by exploiting a characteristic of the actual flow behavior, sets the basis for a meaningful first truncation to which successive approximations contribute only in a relatively minor way. This situation is not expected to change in the nonequilibrium case, which was then analyzed using the preceding ideas. First-truncation nonequilibrium results are discussed in the remainder of this paper.

Received July 1, 1964. This work is part of an investigation carried out under Air Force contract AF 49(638)1280. The author is indebted to M. D. Van Dyke and H. K. Cheng for their helpful suggestions.

* Research Assistant, Department of Aeronautics and Astronautics.

† An alternative to this is the device used by Kao.[2]

Analysis

The gas model that was adopted for chemically relaxing flow consists of a mixture of inert N_2 and reacting oxygen for which the following reactions are considered:

$$O_2 + C \overset{k_c}{\rightleftharpoons} 2O + C$$

where C represents O_2, O, and N_2 with the appropriate rate constant k_c for each reaction. Vibrational degrees of freedom of the diatomic molecules are considered in equilibrium with translation and rotation. Under the previous conditions the chemical state is represented by a single variable, the degree of dissociation α equal to the mass of atomic oxygen divided by the total mass of oxygen. It is felt that this is a simple and yet faithful model for air under conditions such that nitrogen dissociation is negligible.

The flow properties are governed by the physical conservation equations for inviscid, nondiffusive flow, together with the equations of state and chemical rate equation. These equations can be manipulated in a number of ways. Following the reasoning set forth in the introduction, the problem was cast in the form of four partial differential equations for the stream function ψ, the pressure p, the degree of dissociation α, and the temperature T, which were expanded as follows:

$$\psi(r,\theta) = \psi_1(r) \sin\theta + O(\sin^3\theta)$$
$$p(r,\theta) = p_1(r) \cos^2\theta + O(\sin^2\theta)$$
$$\alpha(r,\theta) = \alpha_1(r) \cos^2\theta + O(\sin^2\theta)$$
$$T(r,\theta) = T_1(r) \cos^2\theta + O(\sin^2\theta)$$

The method of truncations then reduces the problem to that of solving a set of four ordinary differential equations for ψ_1, p_1, α_1, and T_1. These equations were solved numerically, employing a standard predictor-corrector machine program. A complete case runs for about 30 sec in the IBM 7090.

Results

Results were obtained for an altitude of 30 km and flight speed of 4.3 km/sec. To the first-truncation approximation, shock wave and body are concentric circular cylinders of radii R and r_b, respectively. Several nonequilibrium regimes were obtained by changing the scale of the flow field. For large R, the chemical relaxation time is small compared with a characteristic flow time, and the flow approaches equilibrium. For small R the reverse is true, and the flow approaches frozen conditions. Typical results are shown in Fig. 2 plotted vs the coordinate $X = R - r$. For present purposes, attention is drawn to the region near the body.

It is not difficult to imagine that, in flows that are nearly frozen with respect to a characteristic flow time, there may be embedded regions where the velocity approaches zero and in which the flow can "unfreeze." One such region is the stagnation point of a blunt body. Here the velocity approaches zero and the local residence time becomes very large as compared with a characteristic flow time. If the ratio of local residence time to chemical relaxation time becomes finite, the nearly frozen approaching flow will react toward equilibrium. Such a reaction does take place near the stagnation point, in a narrow region that might be called the equilibrium layer. A detailed study of this layer is a somewhat more difficult task.

The method of truncations, in dealing with ordinary differential equations, facilitates the study of the equilibrium layer to a large extent. Blunt-body methods that rely on schemes for integration of partial differential equations find the integration mesh size dictated by stability or similar considerations. In contrast, ordinary differential equations can be integrated with high resolution, a decided advantage in investigating localized phenomena such as the stagnation equilibrium layer. However, and in spite of the extremely small step size afforded by the method of truncations, gradients in the equilibrium layer become so large that straightforward integration to the body must stop short of the wall. In order to shed more light on the problem, a new point of view was needed. This was provided by a transformation that changes the role of the variables so that temperature becomes the independent variable. This transformation was found to expose the layer for closer study since, in terms of the new variable, all slopes remain of order one or less through the layer, and integration can be carried out to the wall with high accuracy.

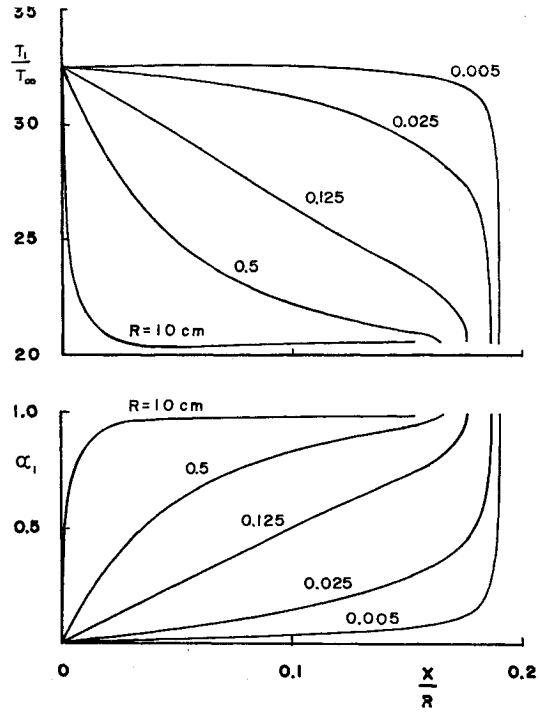

Fig. 2 First-truncation temperature and degree of dissociation for an altitude of 30 km and flight speed of 4.3 km/sec. Values shown are for the stagnation streamline. $X/R = 0$ is at the shock, and all curves end at the body.

Some features of the inner structure of the layer are shown on Fig. 3. In terms of the transformed variables the equilibrium layer appears as a region, very near the body surface, of creeping motion and constant pressure where chemical relaxation proceeds up to final equilibrium at the wall. Inspection of the transformed equations shows that through the layer both velocity and velocity variations are small quantities, and pressure variations are of even higher order.

If the equilibrium layer is defined as the region dominated by large gradients in the temperature, density, and degree of

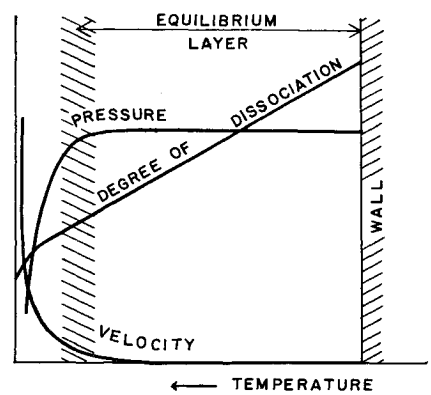

Fig. 3 Qualitative behavior of the flow variables in the equilibrium layer as a function of temperature.

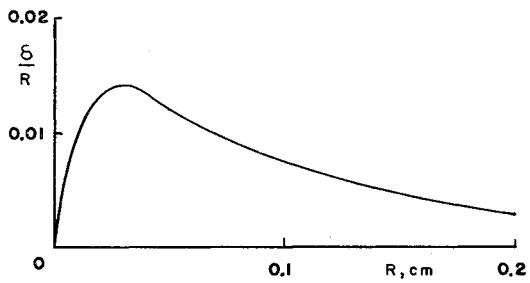

Fig. 4 Equilibrium-layer thickness for edge located where $(dT_1/dX)\ (R/T_\infty) = -100$.

dissociation fields, a thickness for the layer can be defined as the distance from the body surface at which the slope becomes greater than an arbitrarily set value. When this is done, the thickness δ shows a consistent pattern as shown on Fig. 4. The thickness is zero in the frozen limit ($R = 0$), exhibits a maximum somewhere in the nonequilibrium regime, and approaches zero asymptotically in the equilibrium limit ($R \to \infty$). This implies that the surface equilibrium layer is present throughout the entire nonequilibrium regime, with large slopes and large over-all changes near the frozen limit, and still large slopes but vanishing over-all changes as the equilibrium limit is approached (see Fig. 2).

Conclusions and Suggestions for Future Research

Large temperature, density, and degree of dissociation gradients are present near the stagnation region in blunt-body, nondiffusive, nonequilibrium flows in what may be called an equilibrium layer. The dominant features in this layer are small velocity and velocity variations and even smaller (higher-order) pressure variations. This essentially uncouples the dynamics and chemistry of the flow. The equilibrium layer appears, then, as a thin region of constant-pressure chemical relaxation where the degree of dissociation varies almost linearly with temperature. The layer appears to persist throughout the nonequilibrium regime, with vanishing over-all changes in the flow properties as the equilibrium limit is approached, and large over-all changes as the frozen limit is approached. In the frozen limit, the layer has zero thickness and the behavior at the wall could perhaps be analyzed locally by means of the powerful modern techniques for dealing with singular perturbation problems.

It is suggested that the method of truncations may provide a good tool for studying the interaction between viscous effects and the equilibrium layer throughout the nonequilibrium flow regime. A situation to some extent similar to the equilibrium layer occurs in the flow of transparent radiating gases,[3] where the long local residence time near the stagnation point is responsible for the gas radiating all of its energy away. The effect of radiation on the equilibrium layer may be another area of interest for future research.

In the present investigation the equilibrium layer was computed near the stagnation point. Its development and behavior along the body are open to further research.

In near-frozen flows changes in entropy along streamlines are small. However, the stagnation streamline and neighboring streamlines undergo drastic chemical reactions in the equilibrium layer. The subsequent entropy gain is expected to persist along the body in a layer similar to the entropy layer due to bluntness. The study of such a layer may also prove to be of interest for future research.

References

[1] Swigart, R. J., "A theory of asymmetric hypersonic blunt-body flows," Stanford Univ. Rept. SUDAER 120 (January 1962).

[2] Kao, H. C., "A study of viscous hypersonic flow near the stagnation point of a sphere," AIAA Preprint 63-437 (1963).

[3] Thomas, P. D., "On the transparency assumption in hypersonic radiative gas dynamics," AIAA Preprint 64-434 (1964).

Experimental Convective Heat-Transfer Measurements

D. J. Collins* and T. E. Horton†
Jet Propulsion Laboratory,
California Institute of Technology,
Pasadena, Calif.

An extensive series of stagnation-point heat-transfer experiments has recently been completed at the Jet Propulsion Laboratory (JPL). The purpose of these investigations was to determine the range of uncertainties in convective heat transfer due to the limited knowledge of the atmospheres of the near planets. Three atmospheric models were investigated: 9% CO_2, 90% N_2, 1% A; 100% CO_2; and 65% CO_2, 35% A. The Model Atmosphere I is thought to be the most likely composition of the Venus atmosphere. Model Atmosphere II is one of the extremes of the Mars atmosphere. A comparison of these two atmospheres allows general conclusions to be reached regarding carbon dioxide and nitrogen atmospheres. Model Atmosphere III investigated the effect of argon in the Mars atmosphere as indicated by Kaplan.[1] All measurements were made in the JPL hypervelocity shock tube.[2] Calorimeter heat-transfer gages[3] were used on 1- and 2-in. hemispherical cylinders.

The experimental results for Model Atmosphere I are given in Figs. 1 and 2. Since there is only 9% CO_2 present in the mixture, it was thought fruitful to make a comparison with Avco air data.[4] For this particular model atmosphere the convective heat transfer does not differ greatly from that of air. A further comparison is given with General Electric data[5] in Fig. 2 for essentially the same atmosphere (9% CO_2, 91% N_2). Excellent agreement is indicated by the data.

The experimental results for Model Atmosphere II, 100% CO_2, are given in Fig. 3. A comparison is given with the JPL Model I data. The general trend of the 100% CO_2 data is of the order of 10% higher than the 9% CO_2 data. Data from both 2- and 1-in. hemispherical cylinders are shown. It is clear that the data scale as expected. A further comparison with data recently presented by Nerem[6] et al. is given.‡

In Fig. 4 is presented the data for the Model Atmosphere III. It is believed that this is the first experimental data

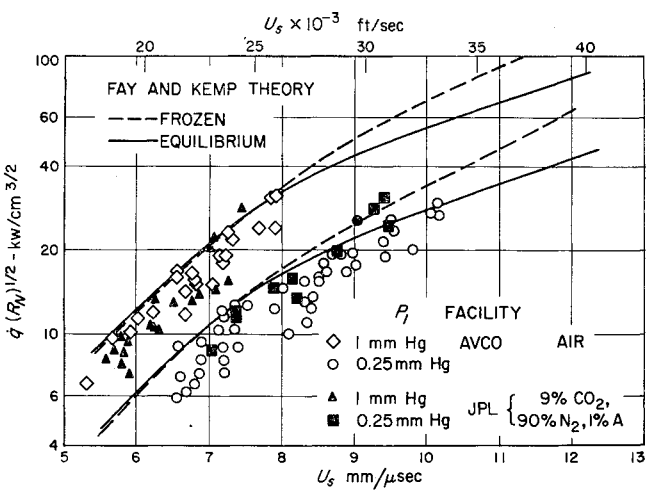

Fig. 1 Comparison of 9% CO_2 data with Avco air data.

Received July 1, 1964.

* Staff Scientist. Member AIAA.

† Senior Research Engineer.

‡ There appears to be a discrepancy between the two graphs presented by Nerem for his CO_2. The graph presenting the final results has been used in this comparison.